

Reliable 4.8 T trapped magnetic fields in Gd-Ba-Cu-O bulk superconductors using pulsed field magnetization

Difan Zhou¹, Jan Srpcic², Kaiyuan Huang², Mark Ainslie², Yunhua Shi², Anthony Dennis², Martin Boll³, and Mykhaylo Filipenko³, David Cardwell², John Durrell²

¹Shanghai Key Laboratory of High Temperature Superconductors, Department of Physics, Shanghai University, Shanghai, 2000444, China

²Department of Engineering, University of Cambridge, Cambridge, CB2 1PZ, UK

³Rolls-Royce Limited & Co. KG, Electrical, Otto-Hahn Ring 6, 81739 Munich, Germany

Email address: dz286@shu.edu.cn
jhd25@cam.ac.uk

Abstract

A robust and reliable *in-situ* magnetization method is essential for exploiting the outstanding magnetic flux trapping ability of bulk superconductors in practical applications. We report a 4.8 T peak trapped magnetic field, B_T , achieved at 30 K in a 36 mm diameter $\text{GdBa}_2\text{Cu}_3\text{O}_{7-\delta}\text{-Ag}$ bulk superconductor using pulsed field magnetization (PFM). To realize this, we have developed a reliable two-step multi-pulse PFM process based on understanding and exploiting the avalanche-like flux jump phenomenon observed in these materials. The magnitude of the applied pulsed magnetic field (B_a) necessary to trap 4.8 T was merely 5.29 T, corresponding to a remarkable magnetization efficiency (B_T/B_a) of 90%.

Introduction

Bulk high temperature superconducting (HTS) materials can trap large magnetic fields and operate effectively as high-strength pseudo-permanent magnets (PMs). Record trapped fields achieved by the field cooling method to date is 17.6 T in a twin-stack of $\text{GdBa}_2\text{Cu}_3\text{O}_{7-\delta}\text{-Ag}$ (GdBCO-Ag) samples [1,2] and 17.24 T in a twin-stack of $\text{YBa}_2\text{Cu}_3\text{O}_{7-\delta}\text{-Ag}$ (YBCO-Ag) samples [3]. The peak trapped field, B_T , surpasses comprehensively the field generated by conventional PMs, *e.g.* NdFeB, at temperatures below 70 K [4-7]. Large, single-grain GdBCO-Ag samples [8] and uranium-doped and irradiated YBCO samples have been shown to exhibit maximum trapped fields exceeding 2 T at liquid nitrogen temperature [9]. Such a high flux density with a significant magnetic field gradient could be transformative for a number of promising applications [10], such as portable high-field magnets [11,12], NMR/MRI [13,14], magnetic drug delivery [15,16], superconducting rotating machines [17] and electromagnetic undulators [18].

In-situ pulsed field magnetization (PFM), which is cost-effective and flexible in application and design compared with quasi-static field cooling (FC) and zero field cooling (ZFC) techniques, would be required to exploit the significance of bulk HTS magnets. However, the critical state model [19] predicts that efficient PFM is not feasible due to the extremely high external magnetic field that is required for magnetic flux to penetrate the pre-cooled superconductor

fully and the heat produced by the rapid flux motion during the magnetization.

Itoh and Yanagi *et al.* investigated thermally assisted flux motion during the PFM process and observed flux jumps, described as “a sudden penetration and rapid motion” of magnetic flux [20]. They later achieved 3.6 T in a 36 mm diameter SmBCO-Ag sample following an IMRA (iteratively magnetizing pulsed field operation with reducing amplitudes) PFM procedure [21]. Fujishiro *et al.* reported the highest trapped field to date of 5.2 T (from an applied field of 6.7 T) in a 45 mm GdBCO-Ag sample [22], and suggested that an “M-shaped” field distribution, obtained from an initial pulse that partially magnetizes the sample, was critical for obtaining such a high trapped field. However, this result has not been reproduced even under very similar conditions [22] and better samples [23]. Weinstein *et al.* recently reported a trapped field of 2 T at 77 K and 4.54 T (deduced from 3.2 T measured 0.7 mm above the sample surface) at 49.1 K in an uranium-doped and irradiated YBCO sample using PFM, and, more importantly, the magnetization efficiency (defined as the ratio between the peak trapped field and applied field, B_T/B_a) was close to 100% [24,25].

Previous reports indicate that a flux jump is an essential condition for obtaining such high trapped fields. We have simulated flux jumps numerically during the PFM process [26] and have extended the classical criterion for a flux jump to occur [27]. Exploiting this phenomenon, we obtained B_T of 4.1 T measured at the surface and 5.3 T measured in-between a stack of two GdBCO-Ag samples of diameter 30 mm. Generally speaking, according to the typical $J_c(B, T)$ characteristics of bulk HTS materials, the critical current density (J_c) and hence the induced shielding current decrease during the ascending period of the pulsed field. An avalanche-like flux jump occurs when the reduction in shielding ability exceeds the increment of B_a , and terminates when a critical state is re-established at the field penetration front. This indicates that a flux jump is prone to occur in a strong pinning scenario. In this paper, we report the PFM of a relatively larger GdBCO-Ag bulk sample than has been achieved previously [27] and an optimised magnetization strategy with a two-step multi-pulse process to routinely achieve a trapped field of 4.8 T.

Experimental details

In the experiment, a 36 mm diameter GdBCO-Ag sample, as shown in figure 1(a), was selected from a batch of melt textured samples prepared using the standard top-seeded melt growth process [28]. Its peak trapped field, magnetized by FC at liquid nitrogen temperature, was 1.2 T. Our state-of-the-art processing technique is able to maintain performance to a sample diameter of over 50 mm [29].

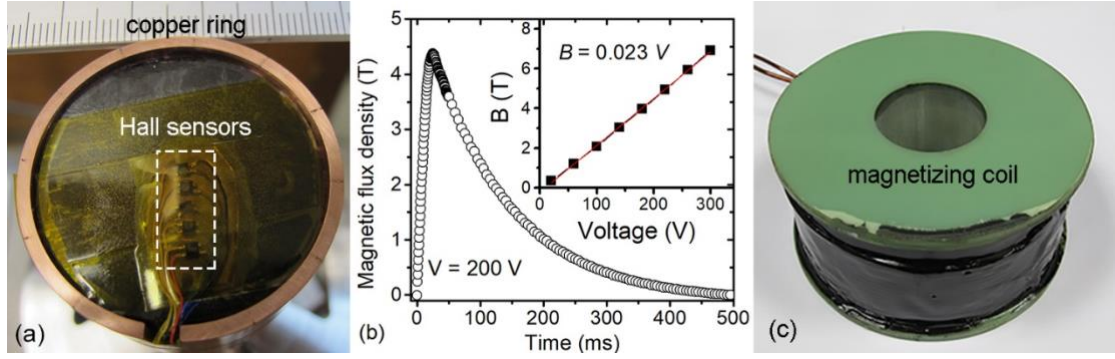


Figure 1. (a) The 36 mm diameter GdBCO-Ag sample under investigation, mounted in a copper holder. (b) Measured magnetic flux density at the centre of the magnetization coil with a discharging voltage of 200 V. The inset shows the dependence of the peak magnetic field of this coil on the charging voltage. (c) copper-wound magnetization coil.

The sample was mounted in a copper holder and cooled conductively using a cryocooler. The temperature was measured using a temperature sensor (Lakeshore Cernox-AA) inserted just beneath the sample in the copper holder. The magnetic field was measured in real time by Hall sensors (Lakeshore model HGT-2101) placed on the surface of the sample with a distance of 2.5 mm between each sensor. The data were recorded initially with a high frequency of 2 kHz for 10 seconds to observe the flux variation during the PFM process, and later with a low frequency of 1 Hz for 15 minutes to allow for sufficient flux creep relaxation.

The pulsed magnetic field was generated in a copper-wound solenoid coil [figure 1(c)] with a flux density proportional to the coil current, and hence proportional to the charging voltage of the capacitor bank. The inset of figure 1(b) shows the pulsed field generated when the charging voltage is 200 V and the dependence of the peak, central magnetic field of the coil on the charging voltage. The rise time of the applied field is around 25 ms and decreases to zero in approximately 500 ms.

Results and Discussion

Our previous work showed that, at any particular operating temperature, there exists a critical magnitude of magnetic field to trigger a flux jump, and here we define this value as B_j . This value of B_j showed very good consistency in repeated experiments, and was found to be insensitive to the geometry of the sample. However, it is different for YBCO, GdBCO and SmBCO samples due to their different intrinsic flux pinning properties [30,31], and varies with the time duration of the pulse and structure of the magnetization coils (solenoid coil, split coils [32,33] and coils with and without iron yoke *etc.* [34]).

Single-pulse PFM experiments were carried out initially in this study. Figure 2 shows the trapped field data at 70 K and 30 K measured 15 minutes after the PFM process to allow for sufficient flux creep relaxation. Significantly, the peak flux density on the central surface of the sample was as high as 4.4 T at 30 K when the applied field was only 4.6 T.

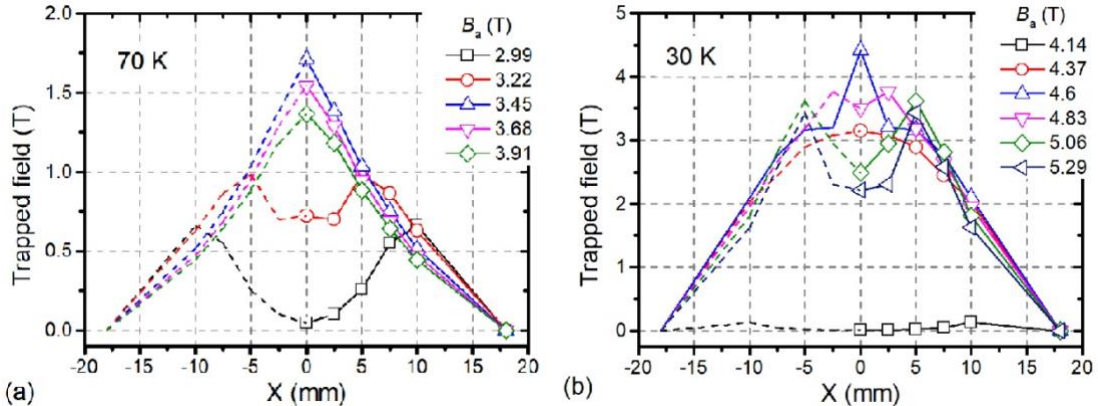


Figure 2. Trapped field profiles at the surface of the bulk GdBCO-Ag sample measured 15 minutes after the PFM process at operating temperatures of (a) 70 K and (b) 30 K. The measured results have been extended using the symmetry of the sample (dashed lines).

Figure 3 shows the dynamic variation of the measured magnetic flux density for different pulsed fields at 30 K. Flux jumps can be observed clearly when B_a exceeds B_j (4.37 T at 30 K), as shown in figure 3 (a) and (b), in contrast to figure 3(c) where the penetration of magnetic flux follows critical state-like behavior. The flux jumps led to an avalanche-like penetration of the magnetic flux until a critical state was re-established at the penetration front, and hence a peak value of trapped field very close to the magnitude of the applied field can be obtained. The magnetic flux density at the centre of the surface of the sample increased above B_a immediately after the flux jump, as shown in figure 3(a), indicating that the magnetic flux fronts “jumped” deeply to the centre of the sample. Further increasing B_a to 5.06 T advanced the initiation of the flux jump by a few milliseconds. A critical state was re-established at a relatively outer location of the sample, resulting in an *M*-shaped trapped field distribution, rather than a conical distribution. It is worth mentioning that the flux creep at the centre of the sample [shown on a logarithmic time scale after the break in figure 3(a)] is negligible after the flux jump. In some cases, the central flux density increases due to the redistribution of the magnetic flux over the sample during this period.

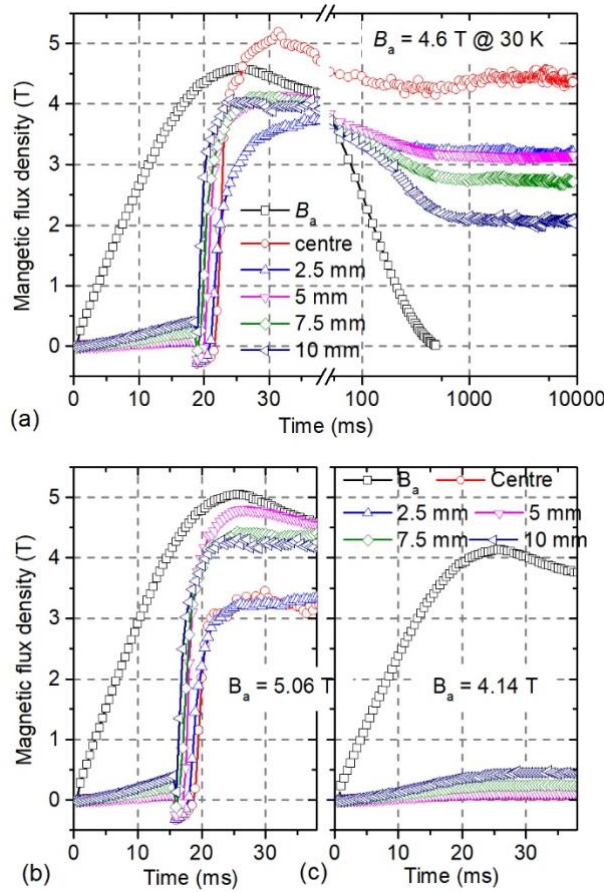


Figure 3. Variation of magnetic flux density measured at the centre of the sample surface at 30 K when the applied pulsed field was (a) 4.6 T, (b) 5.06 T and (c) 4.14 T. A logarithmic time scale is used after the break on the abscissa axis in (a) to illustrate the relaxation of flux creep.

Similar measurements have been repeated at various temperatures, and the dependence of the peak trapped field on the applied field is summarized in figure 4(a), where B_j for each operating temperature can also be determined. The peaks in the respective trapped field profiles were recorded for each measurement. These peaks are observed at positions not coinciding with the centre of the sample at temperatures below 60 K indicating that the magnetic flux front did not reach the centre of the bulk superconductor in these measurements.

The maximum temperature rise (ΔT) of the copper sample holder is summarized in figure 4(b). These observed values of ΔT , which indicate the entire heat generated in the interior of the sample, increase with decreasing operating temperature given that the heat capacity of the material is smaller at a lower temperature. Therefore, further reducing the temperature to 25 K did not improve the trapped field, and an optimal operating temperature exists at around 30 K. On the other hand, the rise in temperature increases linearly with increasing applied field. The occurrence of flux jumps did not affect the observed linearity in ΔT . This indicates that the avalanche-like penetration of flux does not obviously produce heat, which is critical for achieving a high magnetization efficiency.

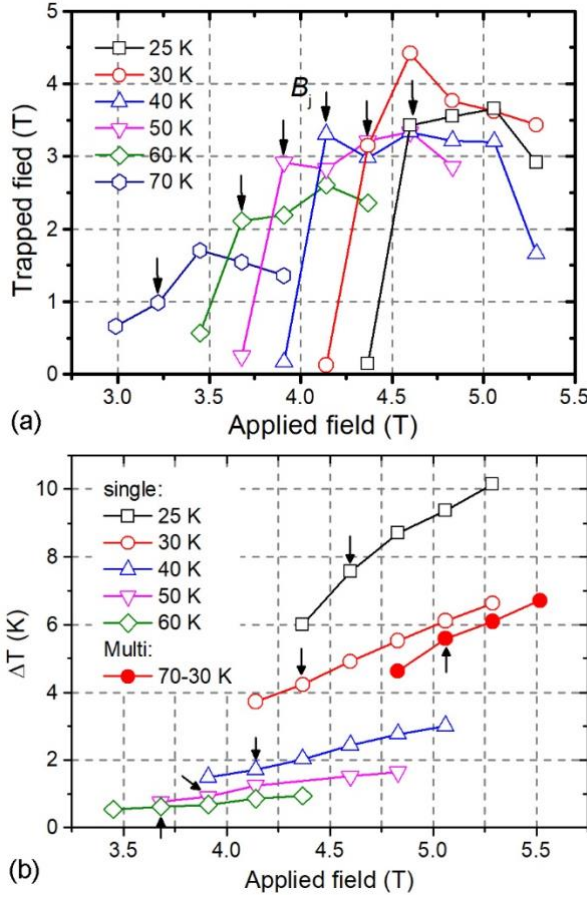


Figure 4. (a) Dependence of the peak trapped field measured on the surface of the sample, and (b) the maximum temperature rise of the copper holder on the magnitude of applied field at each operating temperature. B_j at each temperature is noted by black arrows.

A two-step multi-PFM method was used to further enhance the trapped field [35]. The basic concept is to pre-arrange flux at the periphery of the sample via pre-magnetization at a higher temperature, thus reducing the heat generated during the ascending period of the following pulse at a lower temperature. The maximum peak trapped field of 4.8 T, as shown in figure 5(a), was achieved when a first pulse of 2.99 T was applied at 70 K followed by a second pulse of 5.29 T at 30 K. This peak trapped field of 4.8 T was re-produced in repeated tests with the same conditions and was found to be thermally stable after a long-period decay measurement. However, any change made to these conditions, such as operating temperatures for the first and second pulse or the magnitude(s) of the applied fields, were found to reduce the peak trapped field.

The first pulse of 2.99 T was slightly smaller than the B_j at 70 K which partially magnetized the sample at the periphery where heat was generated [36]. The effect of this two-step method can be evidently found in figure 4(b) where the temperature rise for single- and multi-pulse PFM at 30 K (red open and solid circles) was compared. It allows the applied field to be increased further to 5.29 T at 30 K. The flux jump, as shown in figure 5(b), occurs when B_a approaches its peak value and the penetration front is close to the centre of the sample, resulting in a considerably higher trapped field.

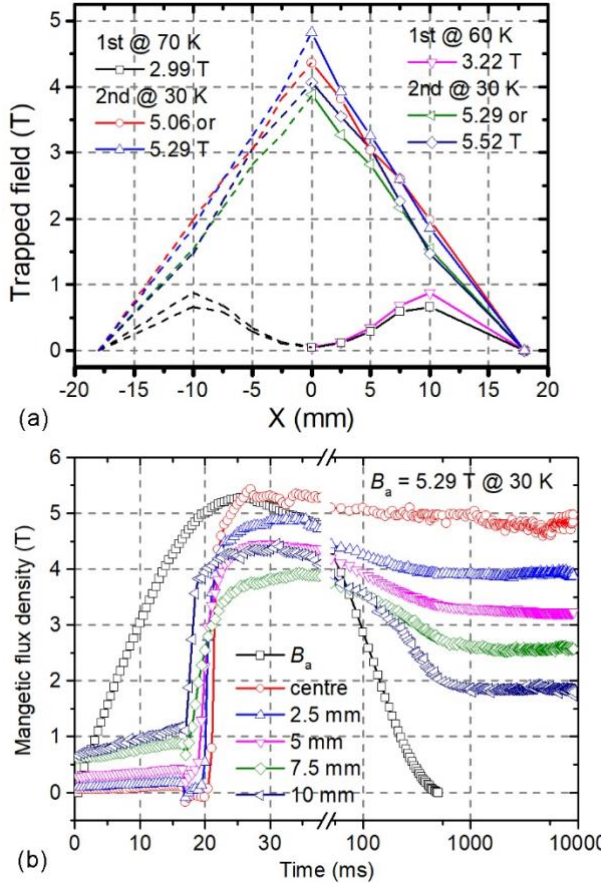


Figure 5. (a) Trapped field profiles achieved via a two-step PFM method with temperature combinations of 70 K + 30 K and 60 K + 30 K measured 15 minutes after the PFM process. (b) Variation of magnetic flux density on the sample surface when $B_a = 5.29$ T was applied at 30 K following an initial pulse of 2.99 T at 70 K.

Conclusions

We have investigated the optimum conditions for pulsed field magnetization of single grain bulk superconductors. Based on our understanding of the flux jump phenomenon, we achieved a peak trapped field of 4.4 T at 30 K from an applied field of 4.6 T using single-pulse PFM process and 4.8 T at 30 K from $B_a = 5.29$ T using a two-step multi-pulse PFM process. The magnetization efficiency was 95% and 90%, respectively. This robust two-step PFM method, which can be summarised as performing the 1st pulse slightly lower than the B_j value at a higher temperature and the 2nd pulse higher than B_j at a lower temperature, is considered a universal approach for achieving high trapped fields for practical applications.

Acknowledgments

This study was supported by the Engineering and Physical Sciences Research Council (No. EP/P00962X/1), the Strategic Priority Research Program of the Chinese Academy of Sciences (No. XDB25000000), the National Key R&D Program (2016YFF0101701) and the project (6140923050202). M D Ainslie would like to acknowledge financial support from an Engineering and Physical Sciences Research Council (EPSRC) Early Career Fellowship, EP/P020313/1.

Data Availability Statement

All data are provided in full in the results section of this paper.

- [1] J. H. Durrell, A. R. Dennis, J. Jaroszynski, M. D. Ainslie, K. G. B. Palmer, Y-H Shi, A. M. Campbell, J. Hull, M. Strasik, E. E. Hellstrom, and D. A. Cardwell, *Supercond. Sci. Technol.* **27**, 082001 (2014)
- [2] K. Huang, Y. Shi, J. Srpočič, M. D. Ainslie, D. K. Namburi, A. R. Dennis, D. Zhou, M. Boll, M. Filipenko, J. Jaroszynski, E. E. Hellstrom, D. A. Cardwell, and J. H. Durrell, *Supercond. Sci. Technol.* **33**, 02LT01 (2020)
- [3] M. Tomita and M. Murakami, *Nature* **421**, 517–20 (2003)
- [4] S. Gruss, G. Fuchs, G. Krabbes, P. Verges, G. Stover, K. Muller, J. Fink, and L. Schultz, *Appl. Phys. Lett.* **79**, 3131-3133 (2001)
- [5] S. Nariki, H. Teshima, and M. Morita, *Supercond. Sci. Technol.* **29**, 034002 (2016)
- [6] O. Vakaliuk, F. Werfel, J. Jaroszynski, and B. Halbedel, *Supercond. Sci. Technol.* **33**, 095005 (2020)
- [7] T. Naito, H. Fujishiro, and S. Awaji, *J. Appl. Phys.*, **126**, 243901(2019)
- [8] S. Nariki, N. Sakai, and M. Murakami, *Supercond. Sci. Technol.* **18**, S126 (2004)
- [9] R. Sawh, R. Weinstein, K. Carpenter, D. Parks, and Kent Davey, Production run of 2 cm diameter YBCO tapped field magnets with surface field of 2 T at 77 K, *Supercond. Sci. Technol.* **26**, 105014 (2013)
- [10] J. H. Durrell, M. D. Ainslie, D. Zhou, P. Vanderbemden, T. Bradshaw, S. Speller, M. Filipenko and D. A. Cardwell, *Supercond. Sci. Technol.* **31**, 103501 (2018).
- [11] T. Oka, Y. Hirose, H. Kanayama, H. Kikuchi, S. Fukui, J. Ogawa, T. Sato, and M. Yamaguchi, *Supercond. Sci. Technol.* **20**, 1233-1238 (2007).
- [12] D. Zhou, M. D. Ainslie, Y. Shi, A. R. Dennis, K. Huang, J. R. Hull, D. A. Cardwell, and J. H. Durrell, *Appl. Phys. Lett.* **110**, 062601 (2017).
- [13] Y. Iwasa, S. Hahn, M. Tomita, H. Lee, and J. Bascunan, *IEEE Trans. Appl. Supercond.* **15**, 2352-2355 (2005)
- [14] K. Ogawa, T. Nakamura, Y. Terada, K. Kose and T. Haishi, *Appl. Phys. Lett.* **98**, 234101 (2011).
- [15] K. Nakagawa, F. Mishima, Y. Akiyama and S. Nishijima, *IEEE Trans. Appl. Supercond.* **22** 4903804 (2012)
- [16] Y. Cha, L. Chen, T. Askew, B. Veal, and J. Hull, *Journal of Magnetism and Magnetic Materials* **311**, 312–317 (2007)
- [17] D. Zhou, M. Izumi, M. Miki, B. Felder, T. Ida and M. Kitano, *Supercond. Sci. Technol.* **25**, 103001 (2012).
- [18] M. Calvi, M. Ainslie, A. Dennis, J. Durrell, S. Hellmann, C. Kittel, D. Moseley, Y. Shi, and K. Zhang, *Supercond. Sci. Technol.* **33**, 014004 (2020)
- [19] C.P. Bean, *Rev. Mod. Phys.* **36**, 31 (1964)
- [20] Y. Itoh, Y. Yanagi and U. Mizutani, *J. Appl. Phys.* **82**, 5600 (1997)
- [21] Y. Yanagi, Y. Itoh, M. Yoshikawa, T. Oka, and U. Mizutani, *Supercond. Sci. Technol.* **18**, 839 (2005).
- [22] H. Fujishiro, T. Tateiwa, A. Fujiwara, T. Oka, and H. Hayashi, *Physica C* **445**, 334 (2006).
- [23] Fujishiro H, Hiyama T, Naito T, Yanagi Y and Itoh Y 2009 *Supercond. Sci. Technol.* **22** 095006
- [24] R. Weinstein, D. Parks, R-P. Sawh, and K. Davey, *J. Appl. Phys.* **126**, 223902 (2019)
- [25] R. Weinstein, D. Parks, R-P. Sawh, K. Carpenter and K. Davey, *Appl. Phys. Lett.* **107**, 152601 (2015).

- [26] M. D. Ainslie, D. Zhou, H. Fujishiro, K. Takahashi, Y. Shi, and J. Durrell, *Supercond. Sci. Technol.* **29**, 124004 (2016).
- [27] D. Zhou, M. D. Ainslie, Jan Srpcic, K. Huang, Y. Shi, A. R. Dennis, D. A. Cardwell, J. H. Durrell, M. Boll and M. Filipenko, *Supercond. Sci. Technol.* **31**, 105005 (2018).
- [28] Y. Shi, D. K. Namburi, W. Zhao, J. H. Durrell, A. R. Dennis, and D. A. Cardwell, *Supercond. Sci. Technol.* **29**, 015010 (2016).
- [29] D. Cardwell, Y. Shi, and D. Numburi, *Supercond. Sci. Technol.* **33**, 024004 (2020)
- [30] D. Zhou, Y. Shi, W Zhao, A. R. Dennis, M. Beck, M. D. Ainsli, K. Palmer, D. A. Cardwell, J. H. Durrell, *IEEE Trans. Appl. Supercond.*, **27**, 6800704 (2017)
- [31] H. Fujishiro, M. Kaneyama, K. Yokoyama, T. Oka, and K. Noto, *Supercond. Sci. Technol.* **18**, 158 (2004)
- [32] E. Morita, H. Matsuzaki, Y. Kimura, I. Ohtani, H. Ogata, M. Izumi, Y. Nonaka, M. Murakami, T. Ida, H. Sugimoto, M. Miki and M. Kitano, *Supercond. Sci. Technol.* **19**, S486 (2006)
- [33] H. Fujishiro, T. Naito and M. Oyama, *Supercond. Sci. Technol.* **24** 075015 (2011)
- [34] M. Ainslie, H. Fujishiro, H. Mochizuki, K. Takahashi, Y. Shi, D. K. Namburi, J. Zou, D. Zhou, A. R. Dennis, and D. A. Cardwell, *Supercond. Sci. Technol.* **29** 074003 (2016)
- [35] M. Ainslie, J. Srpcic, D. Zhou, H. Fujishiro, K. Takahashi, D. Cardwell, J. H. Durrell, *IEEE Trans. Appl. Supercond.* **28**, 6800207 (2018)
- [36] S. Braeck, D. Shantsev, T. Johansen, and Y. Galperin, *J. Appl. Phys.* **92**, 6235 (2002)